

A Comparison of Few-Shot Learning Methods for Underwater Optical and Sonar Image Classification

1st Mateusz Ochal
Heriot-Watt University
Edinburgh, UK
m.ochal@hw.ac.uk

2nd Jose Vazquez
SeeByte
Edinburgh, UK
jose.vazquez@seebyte.com

3rd Yvan Petillot
Heriot-Watt University
Edinburgh, UK
y.r.petillot@hw.ac.uk

4th Sen Wang
Heriot-Watt University
Edinburgh, UK
s.wang@hw.ac.uk

Abstract—Deep convolutional neural networks have shown to perform well in underwater object recognition tasks, on both optical and sonar images. However, many such methods require hundreds, if not thousands, of images per class to generalize well to unseen examples. This is restricting in situations where obtaining and labeling larger volumes of data is impractical, such as observing a rare object, performing real-time operations, or operating in new underwater environments. Finding an algorithm capable of learning from only a few samples could reduce the time spent obtaining and labeling datasets, and accelerate the training of deep-learning models. To the best of our knowledge, this is the first paper to evaluate and compare several Few-Shot Learning (FSL) methods using underwater optical and side-scan sonar imagery. Our results show that FSL methods offer a significant advantage over the traditional transfer learning methods that employ fine-tuning of pre-trained models. Our findings show that FSL methods are not too far from being used on real-world robotics scenarios and expanding the capabilities of autonomous underwater systems.

I. INTRODUCTION

Underwater object recognition is more challenging than in the usual indoor/outdoor environments. Water molecules, dust, and other floating particles cause heavy attenuation of light, distorting the color and introducing haze into optical images. Acoustic sensors are commonly used due to their bigger sensing range compared to other sensing modalities such as optical. Although unaffected by lighting conditions, sonar still greatly suffers from noisy sensor input and lower resolution. Despite these characteristics, state-of-the-art deep convolutional neural networks (DCNN) have shown to perform well on optical [1] and even sonar [2] images.

A key component for achieving good performance is training on large datasets. However, obtaining larger datasets can be expensive and impractical in the marine setting due to the high operational costs of underwater missions, the low abundance of objects, and operational time constraints of missions. All these factors limit the scope of extensive gathering and labeling of large volumes of data. Finding a method that alleviates this problem would be beneficial not only in the underwater research but also to the general robotics community.

The problem of learning with limited data is not novel and has been addressed by a variety of regularisation techniques. One of the popular methods is transfer learning (TL), which has seen general success in the underwater setting [1]. In TL, a network is typically trained on a significantly larger but similar

dataset and later fine-tuned on a smaller dataset. However, TL alone may still require thousands of images in the smaller dataset to generalize reliably.

Over the past several years, there has been a renewed effort in developing more efficient algorithms to perform *Few-Shot Learning (FSL)*. FSL is commonly tackled through meta-learning (e.g MAML [3]) that aims to teach models how to learn from a few samples. Recent efforts have created a range of robust methods and proved to be promising in alleviating the problem of learning with limited data.

While FSL methods have been extensively tested on generic classification datasets, little attention has been given to practical underwater scenarios. In this work, we compare various FSL methods on a collection of underwater optical and sonar datasets. We identify the state-of-the-art and highlight some challenges still faced by FSL methods. Our main contributions can be summarised as follows.

- To the best of our knowledge, our work is the first to compare the performance of several FSL methods for underwater sonar and optical image classification.
- We show that FSL methods offer a significant advantage over the traditional methods of fine-tuning.
- We show that pre-training FSL methods on general-purpose datasets can further improve performance, even when the image types differ significantly.
- We discuss the practicality of using FSL methods in realistic underwater robotics scenarios, highlighting their limitations, and proposing directions for future research.

This paper is structured as follows. We begin with an overview of the related literature in section II, describing the current efforts of training deep learning models with limited data, few-shot learning, and on underwater images. In section III we explain the datasets used for our experiments, before describing the examined methods in section IV and the experimental setup in section V. We report results in section VI, and discuss the limitations of few-shot learning and our experiments in section VII.

II. RELATED WORK

A. Learning with Limited Data

DCNN models can contain well into tens of millions of trainable parameters. As an example, EfficientNet-B7 [4]

which achieves state-of-the-art models on the ImageNet-2012, contains about 66M trainable parameters. It can be generally observed that the more parameters a model has the greater its capacity for learning intricate patterns in data and achieving higher accuracy performance [4].

However, large models can overfit on small training datasets, being unable to learn a correct distribution of data due to the low variance and high bias of the small training set. The problem of overfitting has been addressed by numerous regularisation techniques, such as weight-decay [5], [6], dropout [7], [8], data augmentation [9], transfer learning [10] and many others [11]. A regularisation method can be “*any supplementary technique that aims at making the model generalize better, i.e. produce better results on the test set*” [11].

B. Few-Shot Learning

Few-Shot Learning (FSL) in the context of classification, aims to train models to classify between classes from only a handful of samples. One-shot learning is an extreme case of FSL which utilizes only a single representative from each novel class. In contrast, zero-shot learning aims to learn about novel classes from meta-data (e.g. word descriptions), rather than the samples themselves.

In a k -shot n -way FSL classification task, a model is given k labelled representative images from a collection of n unknown classes, forming a *support set*. The goal is to use the support set to correctly classify a *target set* holding a different set of images from the same n classes. FSL methods typically use a meta-training phase during which the FSL models are pre-trained to learn universal image features as well as learn how to learn. *Set-to-set* training (also called *episodic* training) [12] is a very effective way of meta-training FSL algorithms, where models repeatedly solve batches of FSL classification tasks sampled from a large training set.

The approaches to FSL algorithms can be broadly categorized into three categories: metric-learning, optimization-based, and data augmentation. *Metric-learning* approaches (such as Prototypical Networks [13]–[15]) learn a feature extractor function capable of uniquely describing images from novel classes. *Optimisation-based* approaches (such as MAML [3] and Meta-Learner LSTM [16]) aim to achieve efficient learning through a guided optimisation process on the support set. *Data augmentation* techniques perform affine and color transformations on the support set to create additional data points. For example, [17] exploits an imperfect Generative Adversarial neural network to generate additional negative examples to refine the class boundaries in feature space. The three approaches can be combined taking advantage of two or all three approaches, for example, MAML++ [18].

The current FSL evaluation measures assume a different but similar dataset used during both the evaluation and training of FSL models. As such models are typically trained and evaluated with a single dataset, such as Omniglot [19] for grayscale images and Mini-ImageNet [16] for colored images. However, Omniglot, a hand-written character dataset, and

Mini-ImageNet, a downscaled subset of the generic ImageNet-2012 [20] with only a few underwater classes, that do not generalize well to underwater optical datasets that contain higher levels of noise and color distortion. Moreover, sonar datasets pose a complete domain shift which further impacts the accuracy of algorithms, as is also reflected by our experiments.

C. Underwater Object Classification

Underwater object classification faces many unique challenges poorly represented by datasets such as ImageNet [20]. The quality of optical images underwater is strongly affected by the interactions of light with water molecules and other floating particles. These interactions introduce unique characteristics such as haze, noise (blur and ‘marine snow’ [21]), discoloring, and non-uniform illumination of objects. Combined at various levels of strengths, these factors can make object classification much more challenging to perform.

Additionally, there is a lower abundance of publically-available labeled underwater datasets. Many authors [1], [22]–[25] choose to train neural networks using transfer learning, by fine-tuning last of few layers of pre-trained models, previously trained on larger nonspecialist datasets such as ImageNet [20], and fine-tuned on a specialist underwater dataset. Some authors such as [23] apply rigorous data augmentation including rotation, random cropping, flipping, and color shifting.

Sometimes authors parse datasets using image enhancement methods that aim to restore the true color of objects and remove haze and noise [26]–[29]. Image enhancement techniques are typically used to aid human visibility, and some authors such as [29] show them improving object tracking performance.

Due to the limitation of optical vision, it is common to equip underwater vehicles with a supplementary sonar camera [30]. Imaging sonar has become the widely adopted solution for providing measurements in many practical underwater operations [2], [31]–[33]. It offers significant advantages over optical cameras due to its robustness to water turbidity and variable lighting conditions. A sonar image can be obtained by measuring the time of flight of a pulse-echo sent at various angles. Side-scan sonar (SSS) is particularly popular for surveying and mapping due to its wide coverage and bathymetric capabilities [2]. It can have a range of over a hundred meters. However, the acoustic signal is not perfect and has its limitations. For example, it does not provide any color information and has a lower resolution than optimal images taken with modern cameras. The resolution varies with the distance of detected objects and there is a trade-off between accuracy and range. The random sensor noise, viewing angle dependency and sonar reflection of materials further contribute to the difficulty of working with sonar. As a result, it is common to equip vehicles with both types of sensors that balance out each other’s limitations. Although fusing input signals from both sensory modalities is complex and uncommon, some work successful attempts have been made [30].

Despite the challenging nature of sonar data, [2] has successfully applied a pre-trained ResNet-50 [34] (on ImageNet [20]) for a reliable shipwreck recognition system. [31] has applied a Faster-RCNN [35] with rigorous data augmentation for underwater object detection on both real and simulated sonar images. Transformations on the training set included color inversion, horizontal and vertical flipping, scaling, rotation, and translation.

To the best of our knowledge, only one research paper has applied a single few-shot learning method on underwater sonar images [36]. The authors apply Siamese Networks [37] to two types of submarine objects and six types of surface backgrounds. However, no quantifiable measure of the model (such as accuracy) is reported and there is no comparison made between alternative methods.

III. DATASETS

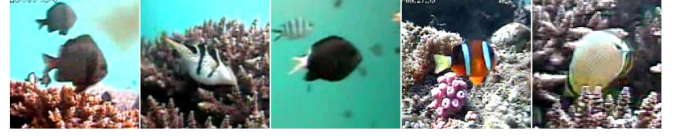
FSL models are typically trained using three disjoint sets of classes: training, evaluation, and testing split. Unlike in classical machine learning, the classes for each split are strictly non-overlapping. Mini-ImageNet [16] is a popular benchmarking dataset for FSL models. It is a downscaled subset of ImageNet-2012 [20] containing only 100 of the original classes. However, this dataset only includes a few underwater classes and no sonar images.

We evaluated the examined methods on two color and two simulated-sonar datasets. Datasets had to meet certain criteria, namely, 1) they had to be of underwater images to fit the scope of this research, 2) contain at least 15 distinct classes, to perform 5-way classification during training, validation, and testing, and 3) contain at least 40 images per classes to fit our experimental setup. For these reasons, we chose the publically-available Fish Recognition dataset [38] and a privately-owned Pipeline Feature dataset containing higher levels of blur and discoloration. From the original 23 classes of the fish dataset, we filtered classes with less than 40 samples. The remaining 19 classes were divided into 9/5/5 classes to be used for training/validation/testing phases, respectively. Similarly, the pipeline dataset, containing 16 classes in total, included 6 classes reserved for training and 5 classes for each of the evaluation phases. All images were scaled to 84 by 84 pixels.

Sonar is integral in many underwater robotics systems. Due to the scarce availability of public sonar datasets, a specialized side-scan sonar (SSS) simulator was used to generate two datasets. As described in [39], the simulator works by ray tracing a 3D Computer-Aided Design (CAD) model to emulate the signal received by a sonar sensor, and thus, producing realistic shadows and highlights of synthetic contacts (objects). We note that the quality of the sonar simulator was validated in experiments with human participants and DCNN networks which were unable to distinguish between real and simulated imagery [39]. We inserted 18 different synthetic contacts into two types of simulated seabeds at various orientations and depth levels. We refer to the two seabed types as *flat* and *rippled*, training algorithms on each type separately, and offering an easier and a more challenging scenario. We used



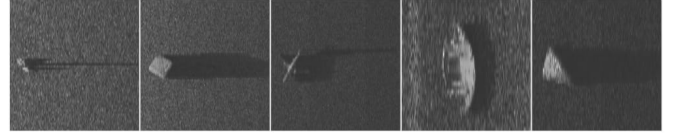
(a) Mini-ImageNet [12], showing a wolf, dog, lipstick, ant, and some fish.



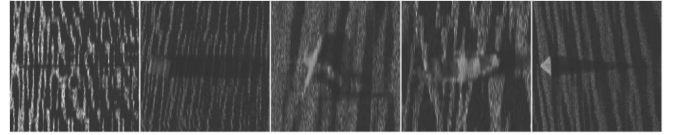
(b) Fish Recognition [38], showing five different fish species.



(c) Pipeline Features include an anode, grout bag, shell, fish and sea urchin.



(d) SSS (flat), showing an anchor, cube, plane, boat, and pyramid.



(e) SSS (rippled), showing an anchor, cube, plane, boat, and pyramid.

Fig. 1. Image examples from the datasets used in this work, representing only a small subset of available classes.

8/5/5 classes per training/validation/testing splits for each type of seabed. To generate the images we cropped an area centered around each object with a large margin around it to include the shadows. Each image was then scaled to 84 by 84 pixels. Figure 1 shows image examples.

IV. METHODOLOGY

In this section, we give a low-level description of FSL methods evaluated in this work: Prototypical Network (PN) [13] and its variants, Consistent Prototypical Networks [15], Soft k-Means ProtoNets [14], Relation Networks [40]. We begin by formally introducing the task of FSL classification and the relevant methods for the fully supervised setting. Then we introduce the semi-supervised setting and the related methods.

A. Fully-supervised few-shot learning definition

Consider the problem of a k -shot n -way classification task sampled from a dataset \mathcal{D} . A model is given a *support set*, $\mathcal{S} = \{(x_1, y_1), \dots, (x_s, y_s)\} \sim \mathcal{D}$, containing n unique classes with k images per class ($|\mathcal{S}| = k \times n$). The goal of the model is to correctly classify a *target set*, $\mathcal{T} = \{(x_1, y_1), \dots, (x_t, y_t)\} \sim$

\mathcal{D} , containing different samples from the same n classes (i.e. $\mathcal{T} \cap \mathcal{S} = \emptyset$). *Set-to-set* training [12] is a popular way to train FSL models, where models are exposed to mini-batches of k -shot n -way classification tasks sampled from a similar but disjoint dataset \mathcal{D}_{train} , where $\mathcal{D}_{train} \cap \mathcal{D} = \emptyset$.

1) **Prototypical Network**: A Prototypical Network [13] computes a representation of the support images for each class and assigns a class of a target image based on its similarity in embedding space. Specifically, support and target images are mapped into a feature space, through a non-linear mapping function $f_\phi : \mathbb{R} \rightarrow \mathbb{R}^M$, parameterized by the trainable parameters ϕ . A class's prototype, $\mathbf{p}_c \in \mathbb{R}^M$, is the mean of the mapped support belonging to a single class:

$$\mathbf{p}_c = \frac{\sum_i f_\phi(x_i) z_{i,c}}{\sum_i z_{i,c}} \quad (1)$$

where $z_{i,c} = 1$ when $y_i = c$ and $z_{i,c} = 0$ when $y_i \neq c$. Given a target point $(x_j, y_j) \in \mathcal{T}$ and a distance function, $d : \mathbb{R}^M \times \mathbb{R}^M \rightarrow [0, +\infty)$, the model computes a similarity between the mapped target point and each of the prototypes. A softmax over the distances produces a probability distribution p over the classes seen in the support set:

$$p(y = c | x_j) = \frac{\exp(-d(f_\phi(x_j), \mathbf{p}_c))}{\sum_{k'} \exp(-d(f_\phi(x_j), \mathbf{p}_{c'}))} \quad (2)$$

The model is trained by minimizing the average negative log-probability:

$$J(\phi) = -\log p(y = y_j | x_j) \quad (3)$$

where y_j is the true class of x_j . Figure 2 shows an intuition of this method.

2) **Relation Network**: A Relation Network [40] augments the original Prototypical Network [13] and replaces the distance measure, d , with a relation module g_φ , parametrized by trainable parameters φ . Specifically, first mapped target points and the prototypes are combined with an operator $h(\mathbf{p}_c, f_\phi(x_j))$ that concatenates each target point with each prototype. Secondly, each of the concatenated vectors are passed through the relation module to produce relation scores, $r_{k,j}$, between a class's prototype, \mathbf{p}_c , and the target image x_j :

$$r_{k,j} = \sum_i x_i g_\varphi(h(\mathbf{p}_c, f_\phi(x_j))) \quad (4)$$

The embedding function f_ϕ and the relation module g_φ are trained end-to-end using the mean squared error (MSE).

B. Semi-supervised few-shot learning definition

In a semi-supervised few-shot classification task, in addition to the labelled support-set, $\mathcal{S} \sim \mathcal{D}$, a model is also given an unlabelled set of images, $\tilde{\mathcal{S}} = \{x_1, \dots, x_{\tilde{s}}\}$, sampled from an unlabelled dataset $\tilde{\mathcal{D}}$. As before, the goal of the model is to correctly classify the target set $\mathcal{T} \sim \mathcal{D}$. The set-to-set training [12] replaces dataset \mathcal{D} and $\tilde{\mathcal{D}}$ with dataset \mathcal{D}_{train} and $\tilde{\mathcal{D}}_{train}$, respectively. Dataset $\tilde{\mathcal{D}}_{train}$ can be the same as \mathcal{D}_{train} , however, without losing generality we keep them separate in notation.

1) Prototypical Network with K-Means Refinement [14]:

This method also augments the original Prototypical Network [13] and refines the prototypes using the unlabelled data $\tilde{\mathcal{S}}$. This method is almost identical to the original with the exception that the prototypes, \mathbf{p}_c , are replaced by the *refined prototype*, $\tilde{\mathbf{p}}_c$, for each class, k . The refinement process uses iterations of soft k-Means algorithms on mapped images from \mathcal{S} and $\tilde{\mathcal{S}}$.

The prototypes \mathbf{p}_c (defined in Eq. 1) act as the initial positions of the cluster centroids (i.e. $\tilde{\mathbf{p}}_c \leftarrow \mathbf{p}_c$). Each labelled example $x_i \in \mathcal{S}^{(X)}$ is given a hard centroid assignment ($z_{i,c} = 1 [y_i = c]$) since their label is considered known and therefore fixed. In contrast, each unlabelled sample \tilde{x}_r is given a partial ('soft') assignment ($\tilde{z}_{r,c}$) to each cluster (of each class k) based on their Euclidean distance to the centroid locations. At each iterative step of the k-means algorithm, the centroids are refined by integrating the adjusted assignments:

$$\tilde{\mathbf{p}}_c = \frac{\sum_i f_\phi(x_i) z_{i,c} + \sum_r f_\phi(\tilde{x}_r) \tilde{z}_{r,c}}{\sum_i z_{i,c} + \sum_r \tilde{z}_{r,c}}, \quad (5)$$

where $\tilde{z}_{r,c} = \frac{\exp(-d(f_\phi(\tilde{x}_r), \tilde{\mathbf{c}}_c))}{\sum_{c'} \exp(-d(f_\phi(\tilde{x}_r), \tilde{\mathbf{c}}_{c'}))}$

Although it is possible to perform multiple iterations of the clustering algorithm, the authors found that the performance does not improve after a single iteration.

a) *Soft K-Means PN + Cluster*: The soft k-means approach described above assumes that $\tilde{\mathcal{S}}$ contains the same classes as \mathcal{S} , but this is unlikely to be true in a practical scenario. Classes that are not part of \mathcal{S} are called *distractors* since they are likely to interfere with the refinement process. To make the method more robust to distractors, the authors introduce an extra cluster that acts as a 'catch-all' cluster for anything that does not belong to the classes of interest, and thus, preventing any distractors from hindering with the refinement. The authors place the cluster at the origin ($\tilde{\mathbf{p}}_c = \mathbf{0}$ for $c > n$) and introduce a learnable length-scale parameter, q_c , that reflects the amount of within-class variation. Thus, the partial assignment is defined as:

$$\tilde{z}_{r,k} = \frac{\exp\left(-\frac{1}{q_k} d(f_\phi(\tilde{x}_r), \tilde{\mathbf{c}}_k) - A(q_k)\right)}{\sum_{k'} \exp\left(-\frac{1}{q_{k'}} d(f_\phi(\tilde{x}_r), \tilde{\mathbf{c}}_{k'}) - A(q_{k'})\right)} \quad (6)$$

where $A(q) = \log(q) + \frac{1}{2} \log(2\pi)$

For simplicity, the authors set $q_{1..C}$ to 1 in their experiments and only learn the length-scale of the distractor cluster q_{n+1} . Our experiments follow the same setup.

b) *Soft K-Means PN + Mask*: The authors consider a second method that deals with distractor classes. Intuitively, a single distractor cluster might not work well with a higher number and diversity of distractors. In a practical situation, the number of distractor classes is likely to be unknown. To address the problems, instead of using a high-variance catch-all cluster, an image is labelled as a distractor if its embedding does not lie within legitimate proximity of any of the class prototypes. Specifically, the soft k-means refinement process

is altered as follows. First, the normalized distances, \tilde{d} , are computed between examples $\tilde{x}_r \sim \tilde{\mathcal{S}}$ and prototypes \mathbf{p}_c :

$$\tilde{d}_{r,c} = \frac{d_{r,c}}{\frac{1}{M} \sum_j d_{r,c}} \quad (7)$$

$$\text{where } d_{r,c} = d(f_\phi(x_r), \mathbf{p}_c) = \|f_\phi(\tilde{x}_r) - \mathbf{p}_c\|_2^2$$

Then, a small neural network is used to compute learnable parameters β_c and γ_c from various statistics of the normalised distances (i.e. using the min, max, variance, skewness and kurtosis of $\tilde{d}_{r,c}$). The parameters β_c and γ_c help to establish how aggressively the unlabelled samples should influence centroids during the refinement process. The final refinement process of *Soft K-Means PN + Mask* method is:

$$\tilde{\mathbf{p}}_c = \frac{\sum_i f_\phi(x_i) z_{i,c} + \sum_r f_\phi(\tilde{x}_r) \tilde{z}_{r,c} m_{r,c}}{\sum_i z_{i,c} + \sum_r \tilde{z}_{r,c} m_{r,c}}, \quad (8)$$

$$\text{where } m_{r,c} = \sigma\left(-\gamma_c \left(\tilde{d}_{r,c} - \beta_c\right)\right)$$

where $m_{r,c}$ are the soft-masks computed by comparing the normalised distances to the learned thresholds.

2) **Consistent Prototypical Network:** Consistent Prototypical Networks (CPNs) [15] are also a semi-supervised FSL method capable of augmenting the original PN [13] and the k-means refined PN [14]. Borrowing from standard semi-supervised learning, the authors use virtual adversarial training (VAT) [41] and random walk (RW) loss [42], [43] to formulate a loss function that drives the set-to-set training process:

$$\mathcal{L}_{SSL} = \mathcal{L}_{VAT} + \mathcal{L}_{RW} \quad (9)$$

Virtual adversarial training loss [41] works on the assumption of *local consistency*, also known as *smoothness*, that two data points which are close together should get similar labels. In other words, if we add small perturbations to a point it should not change its label by much.

The local consistency loss of each point is calculated independently of the other points. Inspired by previous work [42], [43], the authors of Consistent Networks introduce a *global-consistency* loss that considers all data points and the overall structure of the embedding manifold. Let us consider points in the embedding space forming graph structures based on their similarity where the probability of going from a point to another varies based on the similarity of the points. A loss can be calculated through a *random-walk* over these similarity graphs constructed between unlabelled examples and the prototypes. The idea is that a random walker starting from a prototype should rarely cross the natural class decision boundaries, thus, explicitly promoting clustering. This can be achieved by allowing the random walker to take some number of steps jumping between points in the embedding space, and maximizing the probability that the random walker gets back to the initial prototype within those steps.

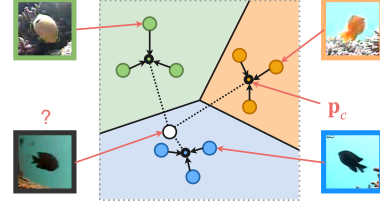


Fig. 2. Prototypical Network. Prototypes p_c are computed as the mean of the support samples belonging to a single class and mapped into an embedding space. A label for a target image is assigned based on the distances to the prototypes.

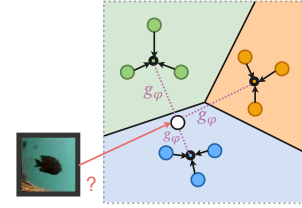


Fig. 3. Relation Network. Prototypes are computed in the same as for Prototypical Networks. However, a label for a target image is assigned based on the score given by the relation module g_ϕ .

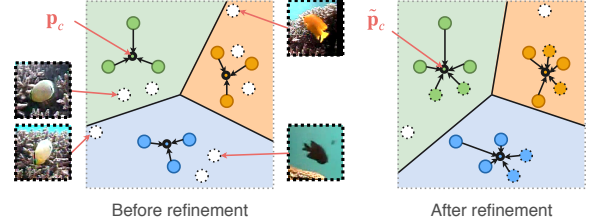


Fig. 4. Prototypical Network with K-Means refinement. Information from unlabelled samples (marked with dashed outlines) is incorporated into the prototypes by a single iteration of soft k-Means. Some samples are omitted in the process due to their low proximity to any prototype.

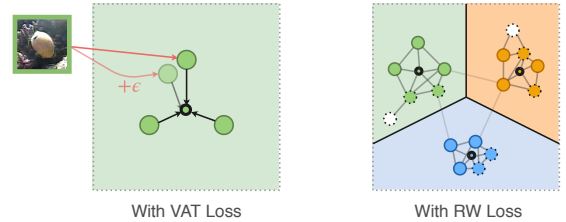


Fig. 5. Consistent Prototypical Networks (CPN). CPN works on top of Prototypical Networks with and without the k-Means refinement. The Cross-Entropy loss is replaced by Virtual Adversarial Training loss (VAT) and Random-Walk loss (RW). During training, VAT adds a small perturbation ϵ to each support sample before mapping it into the embedding space and calculating the prototypes. The goal of RW is to construct a tight neighborhood of samples for each class. This is achieved with the notion of a random walker that transverse a similarity graph between all the prototypes and labeled and unlabelled samples. Starting from a prototype, the random walker should rarely cross the natural class decision boundaries.

V. EXPERIMENTS

A. Training

Three sets of experiments were constructed for each dataset: training¹ on Mini-ImageNet [16], training on one underwater dataset, and training using both datasets:

- 1) **Training on Mini-ImageNet.** To investigate the generalizability of models trained on a general-purpose dataset to underwater datasets, we used Mini-ImageNet [16], following the setup described in the original papers. Specifically, ordinary PN [13] was trained using 5-shot 15-way classification tasks, while all the other methods were trained using 5-shot 5-way tasks. Semi-supervised algorithms drew additional 5 samples per class from the unlabelled partition of the training split. All methods used 5 target images per class. To stabilize training we used mini-batches with 64 tasks. The PN and Relation Networks were trained for 4×10^5 iterations (i.e. mini-batches) and generally converged much sooner. Soft k-Means PNs were trained for 2×10^6 iterations but rarely improved beyond 5×10^5 mini-batches. CPNs were trained for 1.2×10^6 mini-batches. Evaluating on the testing split of Mini-ImageNet showed that our implementations achieved the within 3 accuracy points of the methods' claimed performances.
- 2) **Training on an underwater dataset.** Similarly, we trained the relevant models on underwater datasets but with a few small changes to accommodate the smaller dataset sizes. Ordinary PN [13] were trained using 5-shot 5-way classification to allow for the lower number of classes in the training split. All other methods were trained as before, using 5-shot 5-way tasks. The ordinary PN and Relation Networks were trained using 4×10^3 tasks but we found that the algorithms generally converged much sooner. Soft k-Means PNs and CPNs were trained for 5×10^3 tasks.
- 3) **Training on both datasets.** Using the best models on Mini-ImageNet, we further trained the models on the underwater dataset using the setup described immediately above. As a result, we pre-trained the FSL models on the Mini-ImageNet dataset before training on the underwater dataset.

B. Common evaluation and setup

All experiments follow the same evaluation setup and some common training setup. That is, throughout the training process the models were evaluated on the validation split after every few-thousand iterations, and the best model was saved. At the end of the training, the best model was evaluated on $1000 \times 5\text{-shot } 5\text{-way}$ classification tasks sampled from the testing split of the examined dataset. We repeated each experiment 10 times for each algorithm, dataset, and training type. In contrast to Mini-ImageNet with 100 classes in

¹For all datasets and settings, we mean training exclusively on the training split of the datasets. Similarly, the testing and validation splits were always only used for testing and validation phases, respectively

total, the underwater datasets contained less than 20 classes each. Due to the lower number of classes in underwater datasets, we randomly picked resampled classes to be used for training/testing/validation splits. We reasoned that some FSL methods could learn transferable features from some class combinations more than on others. Therefore, freezing the splits would create a bias towards certain FSL methods, and therefore, we decided to shuffle the classes. Further, we reasoned that the larger number of diversified classes in Mini-ImageNet would be able to average out this effect.

C. Network Architectures

All FSL models used a vanilla convolutional neural network consisting of 4 convolutional blocks. Each block was composed of a convolutional layer (each with 3 by 3 receptive fields, 64 filters, stride 1, and padding 0) followed by batch normalization [44], ReLU activation functions, and max-pooling. ConvNet baseline followed the same setup. Relation Networks used a relation network consisting of two convolutional blocks followed by a linear layer with one output. The ResNet baselines used ResNet-18 and ResNet 50 architectures.

D. Fine-tuned Baselines

In addition to few-shot learning methods, we selected a few fine-tune baselines for comparison. These include a range of convolutional networks trained on the training split of a dataset and then fine-tuning the last layers on the support sets from the evaluation split:

- **ConvNet.** To compare FSL methods with an equally powerful baseline model, we used the same 4 convolutional block architecture as used in the FSL models, with an additional linear layer and softmax over five output units (one for each class in the 5-way FSL task). During training, we trained the whole ConvNet network using a batch size of 64, a learning rate of 0.001, slowly decaying at a rate of 0.9 after each epoch, for 10 epochs. At validation and testing time, we froze the whole but the last linear layer of the network, which was randomly initialized and fine-tuned on the whole support set (25 images for 5-way 5-shot task). Each fine-tuning was performed for 10 iterations with an initialize learning rate of 0.01, and a rapid decay rate of 0.5 after each iteration. For each new evaluation episode, we initialized the last layer with random weights.
- **ResNets.** Similarly to ConvNet, we trained ResNet architectures to test whether a more powerful model would yield higher performance. We used **ResNet-18** and **ResNet-50** trained from random weight initialisation. We also investigated versions of ResNets with a pre-trained set of weights that came with the PyTorch library, obtained from training on full-resolution ImageNet. We refer to the pre-trained variants as **Initialised ResNet-18** and **Initialised ResNet-50**. To accommodate the smaller images size 84 by 84 pixels in the ResNet architecture, we turned off max-pooling layers automatically. Much like with the ConvNet, we trained all four models end-to-end

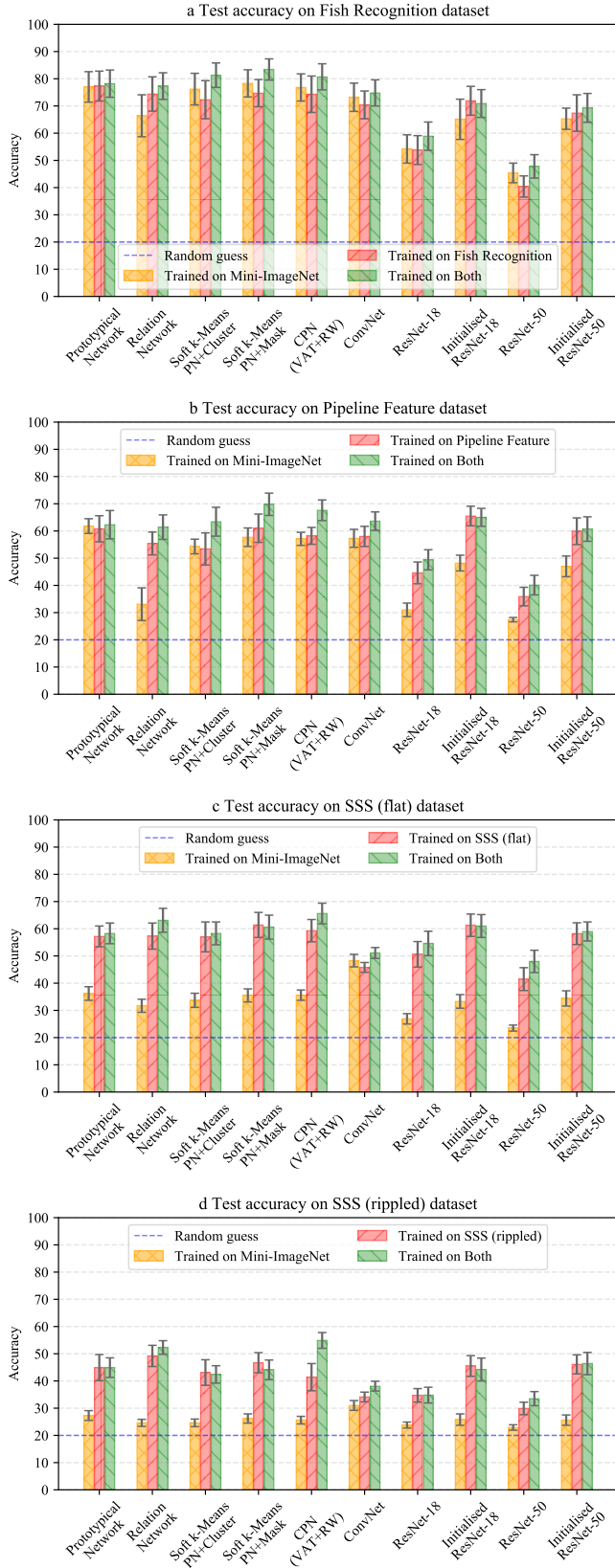


Fig. 6. Test accuracy of models on the testing split of the underwater datasets after training models on the training split of Mini-ImageNet, the underwater dataset, and both datasets. The error bars show a 95% confidence interval.

TABLE I
ACCURACY ON TESTING SPLIT OF FISH RECOGNITION DATASET AFTER TRAINING MODELS ON THE TRAINING SPLIT OF MINI-IMAGE NET (LEFT), FISH RECOGNITION (CENTER), AND BOTH DATASETS (RIGHT).

Method	Mini-ImageNet	Fish Recognition	Both
Prototypical Network	77.0(±5.6)	77.3(±5.5)	78.2(±5.0)
Relation Network	66.4(±7.7)	74.4(±6.3)	77.3(±4.9)
Soft k-Means PN+Cluster	76.2(±5.8)	72.3(±7.0)	81.3(±4.5)
Soft k-Means PN+Mask	78.3(±5.0)	74.7(±5.0)	83.4(±3.9)
CPN (VAT+RW)	76.8(±5.0)	74.3(±6.7)	80.7(±4.8)
ConvNet	73.2(±5.2)	70.4(±5.1)	74.8(±4.8)
ResNet-18	54.2(±5.2)	53.8(±5.3)	58.9(±5.2)
Initialised ResNet-18	65.1(±7.4)	71.9(±5.3)	70.9(±5.1)
ResNet-50	45.4(±3.6)	40.4(±3.9)	47.8(±4.3)
Initialised ResNet-50	65.3(±3.9)	67.4(±6.7)	69.3(±5.3)

TABLE II
ACCURACY ON TESTING SPLIT OF PIPELINE FEATURE DATASET AFTER TRAINING MODELS ON THE TRAINING SPLIT OF MINI-IMAGE NET (LEFT), PIPELINE FEATURE (CENTER), AND BOTH DATASETS (RIGHT).

Method	Mini-ImageNet	Pipeline Feature	Both
Prototypical Network	61.8(±2.7)	60.8(±4.8)	62.3(±5.2)
Relation Network	33.1(±6.0)	55.4(±4.2)	61.4(±4.5)
Soft k-Means PN + Cluster	54.3(±2.7)	53.4(±5.9)	63.4(±5.3)
Soft k-Means PN + Masking	57.7(±3.4)	61.0(±5.2)	69.8(±4.1)
CPN (VAT+RW)	57.1(±2.4)	58.2(±3.1)	67.6(±3.8)
ConvNet	57.3(±3.3)	58.0(±3.7)	63.6(±3.4)
ResNet-18	31.0(±2.5)	44.6(±4.0)	49.4(±3.7)
Initialised ResNet-18	48.2(±2.9)	65.5(±3.6)	65.0(±3.3)
ResNet-50	27.4(±0.8)	35.9(±3.4)	40.1(±3.6)
Initialised ResNet-50	47.0(±3.8)	59.9(±4.9)	60.7(±4.5)

TABLE III
ACCURACY ON TESTING SPLIT OF SSS-FLAT DATASET AFTER TRAINING MODELS ON THE TRAINING SPLIT OF MINI-IMAGE NET (LEFT), SSS-FLAT (CENTER), AND BOTH DATASETS (RIGHT).

Method	Mini-ImageNet	SSS (flat)	Both
Prototypical Network	36.2(±2.5)	57.2(±3.8)	58.3(±3.8)
Relation Network	31.7(±2.4)	57.3(±4.8)	63.1(±4.4)
Soft k-Means PN + Cluster	33.7(±2.6)	57.0(±5.5)	58.3(±4.2)
Soft k-Means PN + Masking	35.5(±2.4)	61.4(±4.6)	60.6(±4.4)
CPN (VAT+RW)	35.6(±1.9)	59.3(±4.1)	65.6(±3.8)
ConvNet	48.3(±2.3)	45.8(±1.8)	51.1(±2.0)
ResNet-18	26.9(±1.9)	50.6(±4.7)	54.6(±4.5)
Initialised ResNet-18	33.3(±2.5)	61.3(±4.1)	61.0(±4.2)
ResNet-50	23.5(±1.1)	41.5(±4.2)	48.0(±4.1)
Initialised ResNet-50	34.4(±2.8)	58.2(±4.0)	59.0(±3.5)

TABLE IV
ACCURACY ON TESTING SPLIT OF SSS-RIPPLED DATASET AFTER TRAINING MODELS ON THE TRAINING SPLIT OF MINI-IMAGE NET (LEFT), SSS-RIPPLED (CENTER), AND BOTH DATASETS (RIGHT).

Method	Mini-ImageNet	SSS (rippled)	Both
Prototypical Network	27.3(±1.8)	44.9(±4.8)	44.9(±3.6)
Relation Network	24.6(±1.3)	49.2(±3.9)	52.3(±2.5)
Soft k-Means PN + Cluster	24.6(±1.4)	43.1(±4.7)	42.4(±3.2)
Soft k-Means PN + Masking	26.2(±1.7)	46.7(±3.7)	44.1(±3.6)
CPN (VAT+RW)	25.6(±1.4)	41.4(±5.0)	54.9(±2.9)
ConvNet	31.0(±1.8)	34.1(±1.8)	38.1(±1.8)
ResNet-18	23.8(±1.1)	34.7(±2.5)	34.8(±2.9)
Initialised ResNet-18	25.8(±2.1)	45.5(±3.8)	44.2(±4.2)
ResNet-50	22.9(±1.0)	29.9(±2.3)	33.5(±2.6)
Initialised ResNet-50	25.6(±1.9)	46.1(±3.5)	46.4(±4.1)

using episodic training and fine-tuning the last layers on the support set. We used a learning rate of 0.0001 to accommodate the higher number of trainable parameters.

VI. RESULTS

The results are presented in Tables I-IV, and Figure 6. Our experiments aim to answer the following questions:

- does training on a general-purpose dataset generalize to underwater datasets?
- is there any advantage in pre-meta-training?
- do FSL methods offer any advantage over traditional fine-tuning methods?
- what is state-of-the-art on underwater optical and sonar datasets?

A. Generalizability of training on Mini-ImageNet

Training on Mini-ImageNet alone generally yielded the worse performance compared to models trained using either of the other two training strategies. An exception to this are methods trained on the Fish Recognition dataset alone. We attribute this to the fact that Mini-ImageNet contains some underwater classes that are very similar in style to Fish Recognition. Additionally, the training split of Mini-ImageNet has more than five times the number of classes than any of the underwater datasets taken individually. These allowed Mini-ImageNet-trained methods to generalize relatively well compared to the testing split of Fish Recognition.

Our results also show that Mini-ImageNet-trained models generalize poorly to sonar. The performance in the more difficult sonar setting (with rippled seabed) is only slightly better than random. The poor performance can be attributed to the significant image domain shift between optical and sonar images. It shows that general-purpose datasets are insufficient to train few-shot learning models where the style of images greatly differs.

B. Advantages of pre-training

Our results show that it is at least as good to train models on both datasets (MiniImageNet and then underwater dataset) as on either of the datasets alone. Interestingly, this is true even for sonar despite the large difference in image style. Some features learned through training on colored images can still generalize to sonar. This finding is particularly useful when there is only a small domain-specific dataset.

In this study, we only explore one way of training on both datasets. However, another way of combining the two datasets would be to mix them into a single dataset and using a weighted loss function to add the cost of the wrong classification on the underwater images. However, we leave this investigation for future work.

C. Advantages of Few-Shot Learning methods

Comparing FSL methods with fine-tuned baselines, across all datasets and training strategies, we observe that in 9 out of 12 settings there is at least one few-shot learning model which achieves higher accuracy than any of the baseline

models. This can be often observed with the ConvNet baseline with an equally powerful backbone model, which indicates that there is a benefit of FSL compared to the traditional method of fine-tuning of pre-trained models. The FSL models even outperform baselines using more powerful backbone architectures such as ResNet-18 and ResNet-50. Interestingly, the pre-trained (initialized) and non-pre-trained ResNet-50 performed worse than the less powerful ResNet-18, suggesting a significant overfit on the training split of datasets due to the increased number of trainable parameters.

On sonar datasets, when models are trained on Mini-ImageNet alone, ConvNet baselines do the best out of all of the methods, outperforming the FSL methods and the more powerful ResNet baselines. We theorize that this superior performance is due to fine-tuning performed during the evaluation which allows the weights of the last layer in the network to be adjusted, which proves superior to the non-tunable evaluation process of the Prototypical Networks and variants. This suggests that the traditional fine-tuning approach is beneficial to perform when the style of images between testing and training greatly differs. It could be interesting to investigate optimization-based FSL methods, however, we leave this for future work.

Further to the setting, the more powerful ResNet baselines also performed fine-tuning, however, their performance was inferior to ConvNet. It is likely that the ResNet networks, which contain many more convolutional layers, learn color-dependent features early in the network which may impede the process of fine-tuning the last few-layers to the style of sonar images. In contrast, ConvNet is a much smaller network and the end vector likely carries much information of the initial sonar input which the fine-tuning process can utilize to quickly adjust to the sonar images.

In other experiments, ResNet baselines do better than the FSL baselines. However, it not fair to compare to these models since the underlying architecture of FSL methods is similar to the ConvNet that contains less trainable parameters and has a shallower architecture. For example, we found that ConvNet contained 1.3×10^5 trainable parameters, whereas were 1.2×10^7 parameters in ResNet-18 and 2.6×10^7 in ResNet-50, which is at two orders of magnitude greater. It would be interesting to substitute FSL models with a more powerful architecture. Work by [45] shows that using a more powerful backbone model in Prototypical Network significantly improves its performance. However, we leave this investigation to future work.

D. State-of-the-art on underwater datasets

Generally, when trained on both datasets, semi-supervised methods tend to do slightly better than the fully supervised FSL methods. This could be due to a combination of at least two reasons. On one hand, the presence of 5 additional unlabelled samples per class exposes the algorithm to more information which it could utilize when learning about new classes. On the other hand, the examined semi-supervised approaches augment the process of calculating class prototypes

which could also be responsible for producing more robust performance. Our supplementary experiments on Soft k-Means PN models with no unlabelled examples suggest that the performance gain exists due to the post-processing of features in the embedding space, rather than the existence of additional unlabelled data. In some experiments, additional data produced worse performance. However, more experiments would need to be collected to offer a more thorough insight, and we leave this investigation for future work.

Interestingly, semi-supervised methods achieved comparable performance to fully supervised methods even though they only used 40% of the labels. In supplementary experiments, we trained the fully-supervised models using only 40% of the data, and we observed an overall decrease in performance in all settings by up to 10 accuracy points compared to when using 100% of the data.

One of the best accuracies on the rippled seabed sonar is achieved by CPN which outperforms all other FSL models by almost a full confidence interval. Our experiments suggest that this advantage is due to the nature of the VAT loss that makes the methods more robust to the noise which is naturally present in the sonar datasets.

VII. DISCUSSION

Throughout the previous sections, we have seen FSL methods performing well on underwater optical and sonar images. In this section, we would like to highlight the significance of our work, as well as some constraints FSL methods, in general, that may require further consideration.

Few-shot learning methods are typically tested under a stringent set of assumptions. In this work, we have evaluated FSL methods loosening one particular assumption where the training and testing datasets come from a similar distribution. We evaluated Mini-ImageNet models on underwater datasets which we found to yield poor performance, especially on sonar. Upgrading the underlying network architecture and the dataset used during training could further improve the performance of our algorithms.

In our experiments, we found that the choice of the support set was essential for achieving strong performance. In practice, the choice of the support set is up to the human operator rather than the FSL methods, which typically assume images to be uniformly sampled from class distributions. However, in real-world applications, the support set is likely to come from a highly correlated stream of video frames. Further investigation is required for performing FSL on video.

Moreover, FSL methods assume objects to be located in the central part of images. In a practical situation, these classification models without modifications are likely to function on top of an automatic target recognition (ATR) system trained to detect object proposals. The ATR system is likely to output a range of regions with a variety of scales and with objects placed anywhere within. This is a further consideration required to apply FSL to work with ATR systems.

Finally, it is typically assumed that all of the support set images are available at once, with no consideration of

future updates. Our future work includes investigating those methods in a continual learning setting where the algorithms are exposed to new classes and samples one sample at a time. It would be interesting for the community to investigate what is a natural saturation level for FSL methods after which there is little or no gain in performance from additional samples and whether there is a natural threshold for switching to the traditional way of fine-tuning once the seen dataset becomes large enough.

VIII. CONCLUSION

In this work, we investigated the use of few-shot learning (FSL) methods in various underwater scenarios. For each method, we compared three meta-training dataset combinations: training on a general-purpose (Mini-ImageNet), on an underwater dataset, and on both datasets. We found that models trained on the general-purpose datasets do not generalize well to underwater optical images that have higher levels of blur and discoloration. We also found that it is generally beneficial to pre-meta-train models on colored datasets before meta-training on optical and even sonar images - despite the large domain-shift between the two modalities. FSL models generally outperform equally powerful baseline models, suggesting a significant advantage over the traditional method of fine-tuning.

In future work, we plan to reduce some assumptions made by FSL methods and investigate these methods working alongside the automatic target recognition systems to create a full few-shot object detector.

ACKNOWLEDGEMENT

We would like to give a special thanks to Antti Karjalainen for generating the simulated side-scan sonar data. This work was supported by the EPSRC Centre for Doctoral Training in Robotics and Autonomous Systems, funded by the UK Engineering and Physical Sciences Research Council and SeeByte Ltd (Grant No. EP/S515061/1).

REFERENCES

- [1] M. Moniruzzaman, S. M. S. Islam, M. Bennamoun, and P. Lavery, "Deep learning on underwater marine object detection: A survey," in *International Conference on Advanced Concepts for Intelligent Vision Systems*, Springer, Cham, 2017, vol. 2.
- [2] J. Rutledge, W. Yuan, J. Wu, S. Freed, A. Lewis, Z. Wood, T. Gambin, and C. Clark, "Intelligent shipwreck search using autonomous underwater vehicles," in *IEEE International Conference on Robotics and Automation (ICRA)*. IEEE, 2018.
- [3] C. Finn, P. Abbeel, and S. Levine, "Model-agnostic meta-learning for fast adaptation of deep networks," *Proceedings of the 34th International Conference on Machine Learning (ICML)*, vol. 70, 2017.
- [4] M. Tan and Q. V. Le, "Efficientnet: Rethinking model scaling for convolutional neural networks," *Proceedings of the 36th International Conference on Machine Learning (ICML)*, 2019.
- [5] D. C. Plaut, "Experiments on learning by back propagation." *Carnegie-Mellon Univ., Pittsburgh, Pa. Dept. of Computer Science.*, 1986.
- [6] K. J. Lang and G. E. Hinton, "Dimensionality reduction and prior knowledge in e-set recognition," *Advances in Neural Information Processing Systems 2 (NIPS)*, 1989.
- [7] G. E. Hinton, N. Srivastava, A. Krizhevsky, I. Sutskever, and R. R. Salakhutdinov, "Improving neural networks by preventing co-adaptation of feature detectors," *arXiv preprint arXiv:1207.0580*, 2012.

- [8] A. Labach, H. Salehinejad, and S. Valaee, "Survey of dropout methods for deep neural networks," *arXiv preprint arXiv:1904.13310*, 2019.
- [9] P. Y. Simard, D. Steinkraus, and J. C. Platt, "Best practices for convolutional neural networks," in *Proceedings of the International Conference on Document Analysis and Recognition (ICDAR)*, 2003.
- [10] S. J. Pan and Q. Yang, "A survey on transfer learning," *IEEE Transactions on Knowledge and Data Engineering*, vol. 22, 2010.
- [11] J. Kukačka, V. Golkov, and D. Cremers, "Regularization for deep learning: A taxonomy," *arXiv preprint arXiv:1710.10686*, 2017.
- [12] O. Vinyals, C. Blundell, T. Lillicrap, K. Kavukcuoglu, and D. Wierstra, "Matching networks for one shot learning," *Advances in Neural Information Processing Systems 29 (NIPS)*, 2016.
- [13] J. Snell, K. Swersky, and R. S. Zemel, "Prototypical networks for few-shot learning," *Advances in Neural Information Processing Systems 30 (NIPS)*, 2017.
- [14] M. Ren, E. Triantafillou, S. Ravi, J. Snell, K. Swersky, J. B. Tenenbaum, H. Larochelle, and R. S. Zemel, "Meta-learning for semi-supervised few-shot classification," *6th International Conference on Learning Representations (ICLR)*, 2018.
- [15] A. Ayyad, N. Navab, M. Elhoseiny, and S. Albarqouni, "Semi-supervised few-shot learning with local and global consistency," *International Journal of Computer Mathematics*, vol. 91, 2019.
- [16] S. Ravi and H. Larochelle, "Optimization as a model for few-shot learning," *5th International Conference on Learning Representations (ICLR)*, 2017.
- [17] R. Zhang, T. Che, Z. Ghahramani, Y. Bengio, and Y. Song, "Metagan: An adversarial approach to few-shot learning," *Advances in Neural Information Processing Systems 31 (NIPS)*, vol. 31, 2018.
- [18] A. Antoniou, H. Edwards, and A. Storkey, "How to train your maml," *arXiv preprint arXiv:1810.09502*, 2018.
- [19] B. M. Lake, R. Salakhutdinov, and J. B. Tenenbaum, "Human-level concept learning through probabilistic program induction," *Science*, vol. 350, 2015.
- [20] O. Russakovsky, J. Deng, H. Su, J. Krause, S. Satheesh, S. Ma, Z. Huang, A. Karpathy, A. Khosla, M. Bernstein, A. C. Berg, and L. Fei-Fei, "ImageNet Large Scale Visual Recognition Challenge," *International Journal of Computer Vision*, vol. 115, pp. 211–252, 2015.
- [21] I. Leonard, A. Arnold-Bos, and A. Alfalou, "Interest of correlation-based automatic target recognition in underwater optical images: theoretical justification and first results," in *Proceedings of SPIE - The International Society for Optical Engineering*, 2010.
- [22] T. Rimavicius and A. Gelzinis, "A Comparison of the Deep Learning Methods for Solving Seafloor Image Classification Task," in *International Conference on Information and Software Technologies*, Springer, Cham, vol. 319, 2017.
- [23] W. Xu and S. Matzner, "Underwater Fish Detection using Deep Learning for Water Power Applications," *5th Annual Conference on Computational Science & Computational Intelligence (CSCI)*, 2018.
- [24] D. Levy, Y. Belfer, E. Osherov, E. Bigal, A. P. Scheinin, H. Nativ, D. Tchernov, T. Treibitz, A. King, and S. M. Bhandarkar, "Automated Analysis of Marine Video With Limited Data," *Proceedings of the IEEE Conference on Computer Vision and Pattern Recognition Workshops (CVPR workshops)*, vol. 1, 2018.
- [25] A. B. Tamou, A. Benzinou, K. Nasreddine, and L. Ballihi, "Underwater Live Fish Recognition by Deep Learning," Springer International Publishing, 2018, vol. 1.
- [26] I. Yoon, S. Jeong, J. Jeong, D. Seo, and J. Paik, "Wavelength-adaptive dehazing using histogram merging-based classification for UAV images," *Sensors (Switzerland)*, vol. 15, 2015.
- [27] P. Sahu, N. Gupta, and N. Sharma, "A Survey on Underwater Image Enhancement Techniques," *International Journal of Computer Applications*, vol. 87, 2014.
- [28] D. Berman, D. Levy, S. Avidan, and T. Treibitz, "Underwater Single Image Color Restoration Using Haze-Lines and a New Quantitative Dataset," *arXiv preprint arXiv:1811.01343*, 2018.
- [29] J. Lu, N. Li, S. Zhang, Z. Yu, H. Zheng, and B. Zheng, "Multi-scale adversarial network for underwater image restoration," *Optics & Laser Technology*, vol. 110, 2019.
- [30] F. Ferreira, D. Machado, G. Ferri, S. Dugelay, and J. Potter, "Underwater optical and acoustic imaging: A time for fusion? a brief overview of the state-of-the-art," in *IEEE OCEANS*, 2016.
- [31] S. Lee, B. Park, and A. Kim, "Deep Learning from Shallow Dives: Sonar Image Generation and Training for Underwater Object Detection," *arXiv preprint arXiv:1810.07990*, 2018.
- [32] C. Barngrover, R. Kastner, and S. Belongie, "Semisynthetic Versus Real-World Sonar Training Data for the Classification of Mine-Like Objects," *IEEE Journal of Oceanic Engineering*, vol. 40, 2015.
- [33] L. Paull, S. Saeedi, M. Seto, and H. Li, "AUV Navigation and Localization: A Review," *IEEE Journal of Oceanic Engineering*, vol. 39, 2014.
- [34] K. He, X. Zhang, S. Ren, and J. Sun, "Deep Residual Learning for Image Recognition," in *2016 IEEE Conference on Computer Vision and Pattern Recognition (CVPR)*. IEEE, 2016.
- [35] S. Ren, K. He, R. Girshick, and J. Sun, "Faster R-CNN: Towards Real-Time Object Detection with Region Proposal Networks," *Advances in Neural Information Processing Systems 28 (NIPS)*, 2015.
- [36] Y. Chen, Q. Ma, J. Yu, and T. Chen, "Underwater acoustic object discrimination for few-shot learning," in *2019 4th International Conference on Mechanical, Control and Computer Engineering (ICMCCE)*, 2019.
- [37] G. Koch, R. Zemel, and R. Salakhutdinov, "Siamese neural networks for one-shot image recognition," in *ICML deep learning workshop*, vol. 2, 2015.
- [38] R. B. Fisher, K.-T. Shao, and Y.-H. Chen-Burger, "Overview of the fish4knowledge project," in *Springer International Publishing*, 2016.
- [39] A. I. Karjalainen, R. Mitchell, and J. Vazquez, "Training and Validation of Automatic Target Recognition Systems using Generative Adversarial Networks," in *IEEE Sensor Signal Processing for Defence Conference (SSPD)*, 2019.
- [40] F. Sung, Y. Yang, L. Zhang, T. Xiang, P. H. S. Torr, and T. M. Hospedales, "Learning to compare: Relation network for few-shot learning," *The IEEE Conference on Computer Vision and Pattern Recognition (CVPR)*, 2017.
- [41] T. Miyato, S.-I. Maeda, S. Ishii, and M. Koyama, "Virtual adversarial training: A regularization method for supervised and semi-supervised learning," *IEEE Transactions on Pattern Analysis and Machine Intelligence*, 2018.
- [42] K. Kamnitsas, D. C. Castro, L. L. Folgoc, I. Walker, R. Tanno, D. Rueckert, B. Glocker, A. Criminisi, and A. Nori, "Semi-supervised learning via compact latent space clustering," *arXiv preprint arXiv:1806.02679*, 2018.
- [43] P. Häusser, A. Mordvintsev, and D. Cremers, "Learning by association - a versatile semi-supervised training method for neural networks," *Proceedings - 30th IEEE Conference on Computer Vision and Pattern Recognition (CVPR)*, vol. 30, 2017.
- [44] S. Ioffe and C. Szegedy, "Batch Normalization: Accelerating Deep Network Training by Reducing Internal Covariate Shift," *International Conference on Machine Learning (ICML)*, 2015.
- [45] B. N. Oreshkin, P. Rodriguez, and A. Lacoste, "Tadam: Task dependent adaptive metric for improved few-shot learning," *Advances in Neural Information Processing Systems 31 (NIPS)*, 2018.